

See discussions, stats, and author profiles for this publication at: <https://www.researchgate.net/publication/236124957>

Carbon Nanotube-Patterned Surface-Based Recognition of Carcinoembryonic Antigens in Tumor Cells for Cancer Diagnosis

ARTICLE in JOURNAL OF PHYSICAL CHEMISTRY LETTERS · APRIL 2013

Impact Factor: 7.46 · DOI: 10.1021/jz400087m

CITATIONS

5

READS

61

9 AUTHORS, INCLUDING:



Gyudo Lee

Harvard University

24 PUBLICATIONS 92 CITATIONS

[SEE PROFILE](#)



Jaemoon Yang

Yonsei University

97 PUBLICATIONS 2,121 CITATIONS

[SEE PROFILE](#)



Kilho Eom

Sungkyunkwan University

65 PUBLICATIONS 759 CITATIONS

[SEE PROFILE](#)

Carbon Nanotube-Patterned Surface-Based Recognition of Carcinoembryonic Antigens in Tumor Cells for Cancer Diagnosis

Taeyun Kwon,^{*,†,‡} Jinsung Park,[¶] Gyudo Lee,^{†,‡} Kihwan Nam,^{†,‡} Yong-Min Huh,^{*,§} Seong-Wook Lee,[⊥] Jaemoon Yang,[§] Chang Young Lee,^{||} and Kilho Eom^{†,#}

[†]Institute for Molecular Sciences, Seoul 120-749, Republic of Korea

[‡]Department of Biomedical Engineering, Yonsei University, Wonju 220-710, Republic of Korea

[¶]Department of Mechanical Engineering, Korea University, Seoul 136-701, Republic of Korea

[§]Department of Radiology, College of Medicine, Yonsei University, Seoul 120-752, Republic of Korea

[⊥]Department of Molecular Biology, Dankook University, Yongin 448-701, Republic of Korea

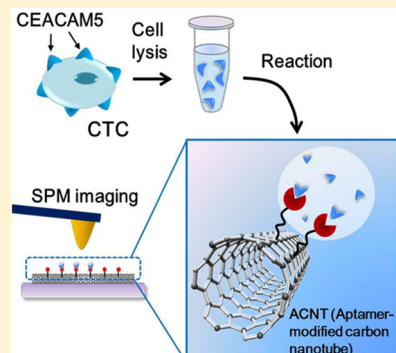
^{||}School of Nano-Bioscience and Chemical Engineering and Interdisciplinary School of Green Energy, Ulsan National Institute of Science and Technology, Ulsan 689-798, Republic of Korea

[#]Biomechanics Laboratory, College of Sport Science, Sungkyunkwan University, Suwon 440-746, Republic of Korea

Supporting Information

ABSTRACT: It has been of high significance to devise a biochemical analytical tool kit enabling the detection of few circulating tumor cells (CTCs) for early diagnosis of cancer. Despite recent effort made to detect few CTCs, it is still challenging to sense such cells with their low concentration and/or the minute amount of marker proteins expressed on few CTCs. In this work, we report the label-free recognition of carcinoembryonic antigens (CEAs) expressed on few CTCs by using a carbon nanotube (CNT) sensor coupled with scanning probe microscopy imaging for cancer diagnosis. It is shown that a CNT-patterned surface is able to specifically capture the CEA molecules in the whole cell lysate of CTCs with their concentration even up to 10^{-3} cells/mL. Our work sheds light on our bioassay based on a CNT-patterned surface for highly sensitive, label-free detection of marker proteins expressed on few tumor cells, which may open a new avenue in early diagnosis of cancer by providing a novel biochemical analysis tool kit.

SECTION: Biophysical Chemistry and Biomolecules



Nanoscale sensors have significantly contributed to the diagnosis of diseases like cancers based on the ability of sensors to capture specific marker proteins that are signatures of specific diseases.¹ Biochemical interaction between marker proteins and a sensor's surface has been measured via an electrochemical or electrical method,² nanomechanical detection,^{3–5} fluorescence analysis,^{6–8} and a microfluidic system.^{9–12} Recently, the detection of marker proteins expressed on cancerous cells has received much interest for effective diagnosis of cancer and monitoring of prognosis after surgical resection.^{13–15} In particular, it is essential to detect carcinoembryonic antigens (CEAs) expressed on circulating tumor cells (CTCs) from a patient's blood sample for the early diagnosis of cancers.^{9,12,16} For cancer diagnosis, it is required to detect minute amounts of CEAs (or CTCs) with their concentrations of ~ 2.5 ng/mL (or 1–10 CTCs per mL).^{17,18} The detection of such CEAs (or CTCs) with their low concentrations has been implemented through an intricate microfluidic chip or a polymerase chain reaction (PCR) that requires a cumbersome process such as signal amplification or labeling.^{9,12,16–21}

In recent years, instead of the aforementioned sensing methods, a scanning probe microscopy (SPM)-based imaging technique has received attention for its capability of label-free detection of marker biomolecules with high sensitivity and high efficiency. For instance, we reported SPM-based label-free recognition of interaction between protein kinases and small molecules (e.g., ATP or drug molecule) at the single-molecule level for drug screening.²² Moreover, it has been recently reported that in order to improve the detection limit of SPM-based sensing, the patterned sensing surface is necessary. Specifically, the patterned sensing surface based on dip-pen lithography²³ or an aligned carbon nanotube (CNT)²⁴ has allowed the sensitive detection of marker proteins with concentrations of < 1 pM. Specifically, the CNT (with its diameter of ~ 4 nm) allows the construction of a minimal sensing area, which results in improving the detection sensitivity even up to 1 pM, as described in our previous

Received: January 14, 2013

Accepted: February 26, 2013

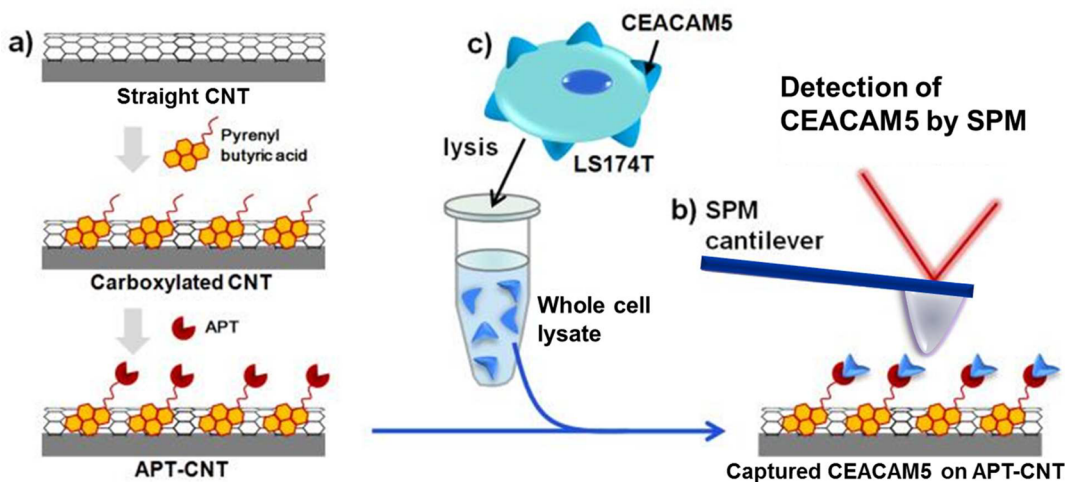


Figure 1. Schematic illustration of (a) the fabrication of a patterned surface based on a carbon nanotube functionalized with an aptamer. (b) SPM-based detection of a marker protein (here, CEACAM5) captured by ACNT. (c) CEACAM5 molecules expressed on CTCs were obtained from the whole lysate of colon cancer LS174T cells.

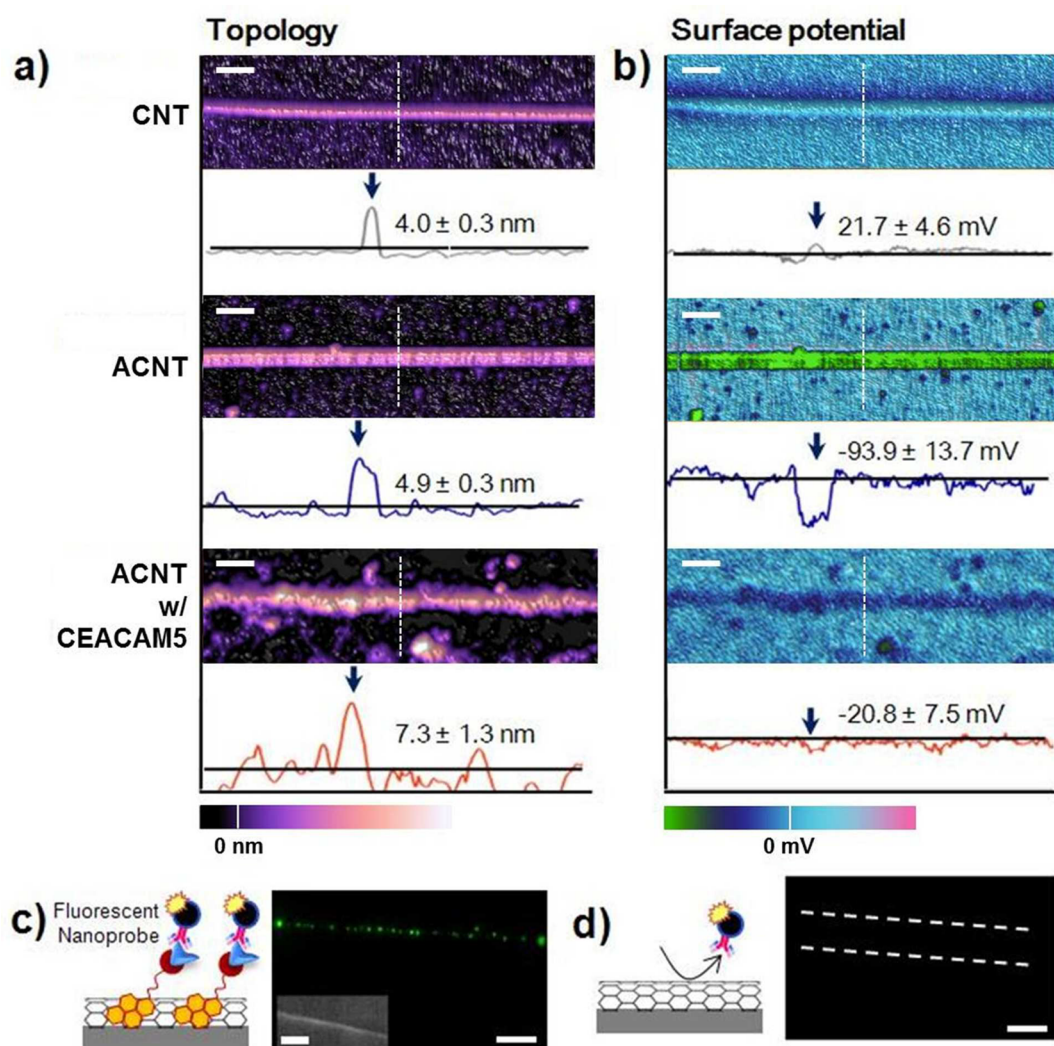


Figure 2. (a) AFM images and (b) KPFM images of a bare CNT, aptamer-functionalized CNT (ACNT), and aptamer-modified CNT capturing CEACAM5 molecules extracted from the LS174T cell lysate (1 cell/mL). (c) Fluorescence image of a secondary antibody bound to CEACAM5 captured by ACNT. Inset shows the scanning electron microscopy image of CNT that capture CEACAM5 proteins labeled with fluorescent nanoprobe. (d) Fluorescence image of a bare CNT treated with a sandwich bioassay. The scale bar is $3 \mu\text{m}$.

work.²⁴ Moreover, the CNT is suitable for functionalization of the receptor molecule, which is essential for the selective detection of specific target molecules using a π -stacking interaction between the CNT and receptor molecule.^{25,26}

In this Letter, we demonstrate the label-free, highly sensitive detection of CEAs expressed on CTCs based on SPM imaging coupled with a CNT-based patterned surface. For fabrication of a CNT-patterned surface, straight carbon nanotubes were chemically grown on a silicon substrate based on chemical vapor deposition process,^{24,27} and subsequently, carbon nanotubes were chemically modified with pyrenyl molecules,²⁴ which led to the chemical functionalization of CNTs with aptamers, which allowed for the specific detection of CEAs. For label-free recognition of CEAs using a CNT-patterned surface, the SPM imaging technique was employed to visualize the CEAs specifically bound to an aligned CNT-based patterned surface (Figure 1). As a model CEA, herein, the carcinoembryonic antigen-related cell-adhesion molecule 5 (abbreviated as CEACAM5, also known as CD66e) from the lysate of LS174T cells was taken into account. Note that CEACAM5 is commonly overexpressed in human colon cancer and plays a role in the key function of cancer cells.^{17,18,21} CEACAM5 is a useful tumor marker to identify recurrences after surgical resection; until recently, a high expression level of CEAs has been detected using the monoclonal antibody.^{9,12,19,21} As described in ref 24, an aptamer is more useful to capture marker proteins than a monoclonal antibody because of the reusability, high binding affinity, and selectivity of the aptamer. Here, we have considered the aptamer as a capturing probe to sense CEACAM5 expressed on cancerous cells (Supporting Information).

Figure 2 depicts the SPM images of a bare CNT-patterned surface, an aptamer-functionalized CNT (ACNT)-patterned surface, and a CEACAM5-bound ACNT-patterned surface. It is shown that the atomic force microscopy (AFM) height of a bare CNT was measured as 4.0 ± 0.3 nm, while the surface potential of a bare CNT is estimated to be 21.7 ± 4.6 mV, which is slightly more positive than that of a Si wafer. After the conjugation of aptamers onto the carboxylated CNT, the height was somewhat increased to 4.9 ± 0.3 nm in comparison with that of the bare CNT. On the other hand, the surface potential was critically decreased to -93.9 ± 13.7 mV, which was ascribed to the negative backbone charge of the aptamer.²⁴ To assess the ability of our ACNT-patterned surface to detect CEACAM5, the lysate of the colon cancer LS174T cell (1 cell/mL) was prepared using a RIPA buffer, and subsequently, the lysate solution was dropped onto the ACNT-patterned surface. It is found that CEACAM5 binding onto the ACNT increases the AFM height by an amount of approximately 2.4 nm, which is attributed to the molecular size of the marker protein CEACAM5, while CEACAM5 binding increases the surface potential by an amount of almost 80 mV because of a charge screening effect due to the isoelectric point of CEA ($pI = 5.74$).²⁰ To validate the specific interaction between ACNT and CEACAM5, we have conducted a negative control experiment, showing that CEACAM5 proteins are not bound to a bare CNT (Figure S1, Supporting Information), which suggests that nonspecific binding of CEACAM5 onto the surface is unlikely to occur. To further confirm the specific binding of CEACAM5 onto ACNT, we have considered the adhesion force imaging, which was obtained simultaneously with AFM topography imaging (Figure S2, Supporting Information). When CEACAM5 molecules were attached to ACNT, CEACAM5-bound

ACNT exhibited a higher adhesion force than a bare CNT due to the chemical interaction between ACNT and CEACAM5.^{28,29}

Moreover, we have conducted the sandwich bioassay in order to verify the specific binding affinity between ACNT and CEACAM5 (Figure 2c and d). In particular, we utilized the CEACAM5 antibody labeled with fluorescent dye as a secondary label for visualizing the CEACAM5 proteins bound to ACNT. Figure 2c shows that CEACAM5 proteins (bound to a secondary label shown as a green dot) are specifically bound to ACNT. However, the sandwich bioassay possesses a restriction on visualizing and quantifying a single CEACAM5 protein bound to ACNT, which is ascribed to an optical limit at the visible light field. In addition, the sandwich bioassay using a bare CNT confirms that nonspecific binding of CEACAM5 onto a bare surface is unlikely to happen (Figure 2d).

We have also investigated the potential of our ACNT-patterned surface for CTC detection at the single cell level. Here, instead of cell lysates, the solution containing LS174T cells (as a model CTC) was dropped onto an ACNT-patterned surface. The nucleus-stained LS174T cells bound to CNT were visualized by fluorescence imaging (Figure S3a, Supporting Information). The expression of CEACAM5 proteins on LS174T cells bound to CNT was verified by sandwich bioassay (Figure S3b, Supporting Information). It is shown that our ACNT-patterned surface is able to effectively capture a single tumor cell in a solution of 1 mL. For the early diagnosis of cancer, it is more favorable to detect CEACAM5 expressed on few tumor cells with their low concentration, that is, $\ll 1$ cell/mL.

Now, we have scrutinized the detection limit of our ACNT-patterned surface for sensing CEACAM5 proteins expressed on CTCs. Here, we consider the ACNT-patterned surface treated with the solution containing LS174T cells with a concentration of 10^{-3} –1 cells/mL for 1 h. It is shown that as the CTC concentration increases, so does the roughness change due to CEACAM5 proteins bound to CNT (Figure 3a). The number

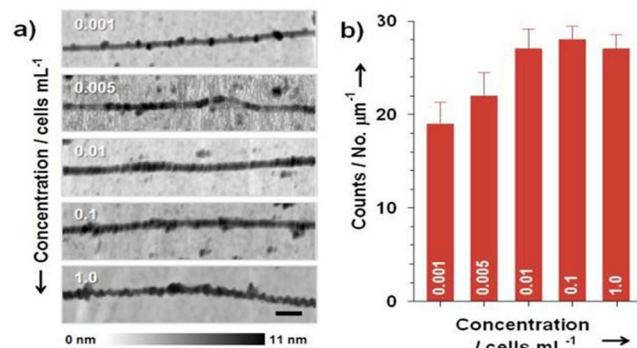


Figure 3. Quantitative characterization for the detection sensitivity of a CNT-patterned surface: (a) topology images and (b) the number of CEACAM5 proteins bound to a functionalized CNT as a function of CTC concentrations. The scale bar is 100 nm.

of CEACAM5 proteins bound to CNT per unit length of the CNT as a function of CTC concentration is provided in Figure 3b. Here, enumeration of CEACAM5 proteins is implemented using AFM images of the CNT that capture CEACAM5 proteins. It is interestingly found that even in the CTC concentration of 10^{-3} cells/mL, the number of CEACAM5 proteins bound to the CNT is measured to be 18.3 ± 3.2

proteins per unit length (i.e., 1 μm) of the CNT. When the CTC concentration is larger than 10^{-2} cells/mL, the number of proteins bound to the CNT saturates. This suggests that our CNT-patterned surface is useful in the label-free detection of marker proteins expressed on few tumor cells with a concentration of much less than 1 cell/mL, which shows that the detection sensitivity of our ACNT-based sensor is much higher than that of other sensing methods.

To gain insight into the binding affinity between our ACNT-based sensor and marker protein (CEACAM5), we have measured the number of marker proteins bound to the CNT as a function of time based on the cell lysate prepared with a CTC concentration of 1 cell/mL. Figure 4a shows the SPM images of

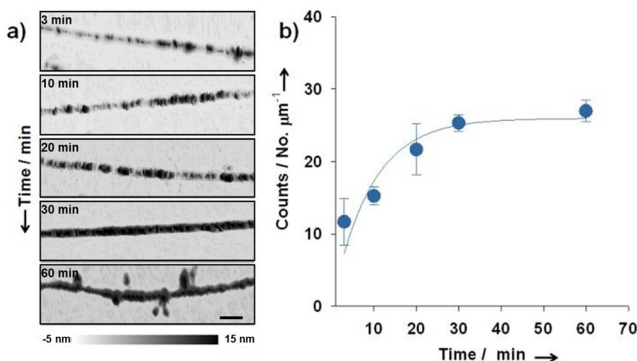


Figure 4. Characterization of the kinetics of binding between a functionalized CNT and CEACAM5 proteins: (a) topology images of a functionalized CNT treated with the whole lysate as a function of time and (b) the number of CEACAM5 molecules captured by a functionalized CNT. The scale bar is 100 nm.

a CNT-based sensor interacting with marker proteins as a function of time. It is shown that the roughness of the CNT is increasing with respect to time, which is attributed to the binding of marker proteins onto the CNT. Figure 4b depicts the number of marker proteins bound to the CNT per unit length of the CNT as a function of time. It is interestingly found that the marker proteins were captured by our ACNT-based sensor within 20 min, which may be due to the high binding affinity between our sensor and marker protein. The kinetics of binding between our sensor and marker protein can be described by Langmuir kinetics, which suggests that the number of marker proteins bound to our sensor is given by $N(t) = N_0[1 - \exp(-k_b t)]$, where N_0 is the equilibrium value of the number of marker proteins bound to the CNT and k_b is a kinetic rate for binding between the CNT and marker protein. We have found that the kinetic rate is estimated to be $0.06 \pm 0.02 \text{ min}^{-1}$. It is implied that our method enables the tactile sensation of marker proteins, at single-molecule resolution, expressed on few tumor cells. A previous study¹⁶ reported the PCR-based detection of CEACAM5-mRNA as a prognostic marker by using a sample of peripheral blood. On the other hand, the detection sensitivity of our ACNT-based sensor is higher than that of PCR-based detection for sensing CEACAM5, and our method does not require any amplification or labeling process that is usually necessary for PCR-based sensing. Moreover, it should be noted that CEACAM5, instead of mRNA, is a principal agent responsible for an oncogenic signaling in intestinal cancer because the mRNA level is not always correlated with the protein level due to the complex translational mechanism in cancer cells.¹⁶

In conclusion, we have developed the ACNT-patterned surface coupled with SPM imaging, which allows the label-free detection of CEAs expressed in few tumor cells for cancer diagnosis. It is shown that our sensing method is able to detect not only a single CTC but also CEAs expressed on few CTCs with a concentration of <1 cell/mL. In particular, our sensing method enables the recognition of CEA proteins even at single-molecule resolution. Moreover, our sensor is able to provide quantitative insight into the binding kinetics of CEA to the aptamer (functionalized on the CNT). Our study may be applicable for studying not only the biomolecular interactions that play a role in oncogenic signaling but also a precise prognosis of cancer recurrence and metastasis leading to cancer diagnosis.

ASSOCIATED CONTENT

Supporting Information

The experimental methods, including straight CNT growth, fabrication of the sensing substrate, the bioassay, tapping mode AFM, KPFM imaging, and preparation of the fluorescence experiment, as well as topology images and schematic illustrations of fluorescence microscopic images are described. This material is available free of charge via the Internet at <http://pubs.acs.org>.

AUTHOR INFORMATION

Corresponding Author

*E-mail: tkwon@yonsei.ac.kr (T.K.); ymhuh@yuhs.ac (Y.-M.H.).

Author Contributions

T.K., Y.-M.H., and K.E. designed the research. J.P., G.L., and K.N. performed the experiments. T.K., J.P., J.Y., Y.-M.H., S.-W.L., C.Y.L., and K.E. analyzed the experimental data. T.K., J.P., G.L., J.Y., and K.E. wrote the manuscript. All authors contributed to this work.

Notes

The authors declare no competing financial interest.

ACKNOWLEDGMENTS

This work was supported by the Nation Research Foundation of Korea (NRF) under Grants NRF-2010-0009428, 2012R1A1B3002706, and 2012R1A1A2008616.

REFERENCES

- Arlett, J. L.; Myers, E. B.; Roukes, M. L. Comparative Advantages of Mechanical Biosensors. *Nat. Nanotechnol.* **2011**, *6*, 203–215.
- Patolsky, F.; Zheng, G.; Lieber, C. M. Nanowire-Based Biosensors. *Anal. Chem.* **2006**, *78*, 4260–4269.
- Eom, K.; Park, H. S.; Yoon, D. S.; Kwon, T. Nanomechanical Resonators and Their Applications in Biological/Chemical Detection: Nanomechanics Principles. *Phys. Rep.* **2011**, *503*, 115–163.
- Lee, G.; et al. Real-Time Quantitative Monitoring of Specific Peptide Cleavage by a Proteinase for Cancer Diagnosis. *Angew. Chem., Int. Ed.* **2012**, *51*, 5837–5841.
- Datar, R.; Kim, S.; Jeon, S.; Hesketh, P.; Manalis, S.; Boisen, A.; Thundat, T. Cantilever Sensors: Nanomechanical Tools for Diagnostics. *MRS Bull.* **2009**, *34*, 449–454.
- Lee, S.; et al. Polymeric Nanoparticle-Based Activatable Near-Infrared Nanosensor for Protease Determination In Vivo. *Nano Lett.* **2009**, *9*, 4412–4416.
- Lee, J.-H.; Kim, E. S.; Cho, M. H.; Son, M.; Yeon, S.-I.; Shin, J.-S.; Cheon, J. Artificial Control of Cell Signaling and Growth by Magnetic Nanoparticles. *Angew. Chem., Int. Ed.* **2010**, *49*, 5698–5702.

- (8) Park, J.; et al. Anchored Proteinase-Targetable Optomagnetic Nanoprobes for Molecular Imaging of Invasive Cancer Cells. *Angew. Chem., Int. Ed.* **2012**, *51*, 945–948.
- (9) Wang, S.; et al. Highly Efficient Capture of Circulating Tumor Cells by Using Nanostructured Silicon Substrates with Integrated Chaotic Micromixers. *Angew. Chem., Int. Ed.* **2011**, *50*, 3084–3088.
- (10) Lee, G.; et al. Electrochemical Detection of High-Sensitivity CRP Inside a Microfluidic Device by Numerical and Experimental Studies. *Biomed. Microdevices* **2012**, *14*, 375–384.
- (11) Yager, P.; Edwards, T.; Fu, E.; Helton, K.; Nelson, K.; Tam, M. R.; Weigl, B. H. Microfluidic Diagnostic Technologies for Global Public Health. *Nature* **2006**, *442*, 412–418.
- (12) Nagrath, S.; et al. Isolation of Rare Circulating Tumour Cells in Cancer Patients by Microchip Technology. *Nature* **2007**, *450*, 1235–1239.
- (13) Visvader, J. E. Cells of Origin in Cancer. *Nature* **2011**, *469*, 314–322.
- (14) Eaves, C. J. Cancer Stem Cells: Here, There, Everywhere? *Nature* **2008**, *456*, 581–582.
- (15) Hanash, S. M.; Pitteri, S. J.; Faca, V. M. Mining the Plasma Proteome for Cancer Biomarkers. *Nature* **2008**, *452*, 571–579.
- (16) Vardakakis, N.; et al. Prognostic Significance of the Detection of Peripheral Blood CEACAM5mRNA-Positive Cells by Real-Time Polymerase Chain Reaction in Operable Colorectal Cancer. *Clin. Cancer Res.* **2011**, *17*, 165–173.
- (17) Miller, M. C.; Doyle, G. V.; Terstappen, L. W. M. M. Significance of Circulating Tumor Cells Detected by the CellSearch System in Patients with Metastatic Breast Colorectal and Prostate Cancer. *J. Oncol.* **2010**, *2010*.
- (18) Aggarwal, C.; et al. Relationship among Circulating Tumor Cells, CEA and Overall Survival in Patients with Metastatic Colorectal Cancer. *Ann. Oncol.* **2013**, *24*, 420–428.
- (19) Konstantopoulos, K.; Thomas, S. N. Cancer Cells in Transit: The Vascular Interactions of Tumor Cells. *Annu. Rev. Biomed. Eng.* **2009**, *11*, 177–202.
- (20) Scorilas, A.; Chiang, P. M.; Katsaros, D.; Yousef, G. M.; Diamandis, E. P. Molecular Characterization of a New Gene, CEAL1, Encoding for a Carcinoembryonic Antigen-Like Protein with a Highly Conserved Domain of Eukaryotic Translation Initiation Factors. *Gene* **2003**, *310*, 79–89.
- (21) Thomas, S. N.; Zhu, F.; Schnaar, R. L.; Alves, C. S.; Konstantopoulos, K. Carcinoembryonic Antigen and CD44 Variant Isoforms Cooperate to Mediate Colon Carcinoma Cell Adhesion to E- and L-Selectin in Shear Flow. *J. Biol. Chem.* **2008**, *283*, 15647–15655.
- (22) Park, J.; et al. Single-Molecule Recognition of Biomolecular Interaction via Kelvin Probe Force Microscopy. *ACS Nano* **2011**, *5*, 6981–6990.
- (23) Lee, K.-B.; Kim, E.-Y.; Mirkin, C. A.; Wolinsky, S. M. The Use of Nanoarrays for Highly Sensitive and Selective Detection of Human Immunodeficiency Virus Type 1 in Plasma. *Nano Lett.* **2004**, *4*, 1869–1872.
- (24) Nam, K.; et al. Aptamer-Functionalized Nano-Pattern Based on Carbon Nanotube for Sensitive, Selective Protein Detection. *J. Mater. Chem.* **2012**, *22*, 23348–23356.
- (25) Chen, R. J.; Bangsaruntip, S.; Drouvalakis, K. A.; Wong Shi Kam, N.; Shim, M.; Li, Y.; Kim, W.; Utz, P. J.; Dai, H. Noncovalent Functionalization of Carbon Nanotubes for Highly Specific Electronic Biosensors. *Proc. Natl. Acad. Sci. U.S.A.* **2003**, *100*, 4984–4989.
- (26) Chen, R. J.; Zhang, Y.; Wang, D.; Dai, H. Noncovalent Sidewall Functionalization of Single-Walled Carbon Nanotubes for Protein Immobilization. *J. Am. Chem. Soc.* **2001**, *123*, 3838–3839.
- (27) Hong, B. H.; Lee, J. Y.; Beetz, T.; Zhu, Y.; Kim, P.; Kim, K. S. Quasi-Continuous Growth of Ultralong Carbon Nanotube Arrays. *J. Am. Chem. Soc.* **2005**, *127*, 15336–15337.
- (28) Lee, G.; Lee, H.; Nam, K.; Han, J.-H.; Yang, J.; Lee, S. W.; Yoon, D. S.; Eom, K.; Kwon, T. Nanomechanical Characterization of Chemical Interaction between Gold Nanoparticles and Chemical Functional Groups. *Nanoscale Res. Lett.* **2012**, *7*, 608.
- (29) Berger, C. E. H.; van der Werf, K. O.; Kooyman, R. P. H.; de Groot, B. G.; Greve, J. Functional Group Imaging by Adhesion AFM Applied to Lipid Monolayers. *Langmuir* **1995**, *11*, 4188–4192.